ELSEVIER

Journal of Hazardous Materials 57 (1998) 127–144

JOURNAL OF HAZARDOUS MATERIALS

Simulation of acid washing of municipal solid waste incineration fly ashes in order to remove heavy metals

B. Van der Bruggen *, G. Vogels, P. Van Herck, C. Vandecasteele

Department of Chemical Engineering, University of Leuven, de Croylaan 46, Heverlee B-3001, Belgium

Received 19 February 1997; accepted 29 May 1997

Abstract

Fly ash from municipal waste incinerators constitutes an environmental problem, as it is polluted with heavy metals. By extracting the heavy metals from fly ashes with an acid solution, they can be partly removed and possibly recovered. The remaining fly ash can be landfilled or used as construction material. In this paper, the results of experimental leaching tests of fly ash are compared with computer calculations of the thermodynamic equilibrium of the leaching solution —fly ash system. The computer program MINTEQA2, used for this purpose, allows to predict the metal concentrations in the leaching solution, the minerals that precipitate, and the pH of the leaching solution at equilibrium. A calculation approach was chosen, whereby the simulation of the complex leaching process was divided into five subproblems. A leaching diagram with linear scales was introduced to visualise the equilibria as a function of pH. The computer simulation was used in two applications: calculation of the impact of addition of a complexing agent on the leaching behaviour of lead, and optimisation of the volume of liquid to be used in the leaching process for a given amount of fly ash. © 1998 Elsevier Science B.V.

Keywords: Heavy metals; Leaching; Fly ash; Modelling; MINTEQA2

1. Introduction

In Flanders, Belgium, around 2.8 million tonnes of municipal waste is generated yearly, of which 30% is selectively collected; 43% of the rest fraction is processed in

* Corresponding author.

PII S0304-3894(97)00078-2

incinerators and 57% is landfilled [1]. Incineration of one tonne of municipal waste leads to the formation of 10 to 50 kg of fly ash depending on the type of incinerator. Combustion residues in general, and fly ash in particular, form a major environmental problem. This fly ash is contaminated with heavy metals and polychlorinated dibenzodioxins and dibenzofurans. It must be considered as hazardous according to the Flemish environmental legislation [2].

Generally, dust particles are removed from the incinerator flue gas by means of an electrostatic precipitator. Wet scrubbers remove in a first stage HCl and HF from the flue gas and, in a second stage, SO_2. The first stage produces an acid waste water mainly containing HCl and to a lesser extent HF. This acid solution can be used, e.g. to leach the fly ash, in order to remove part of the heavy metals, as in the 3R process developed in the Karlsruhe Nuclear Research Centre [3]. Of course, other (waste) acid solutions can in principle be used for the same purpose. The aim can be twofold: obtain a waste material containing a smaller amount of heavy metals so that it can be used as a construction material [4] or landfilled under less stringent conditions; and recover some heavy metals.

In this paper, a study is made of the acid (HCl) extraction process as a treatment method for fly ash from a municipal waste incinerator in order to remove the leachable fraction of the heavy metals, as described in Refs. [5,6]. Leaching with a HCl solution simulates leaching with wash water from the wet scrubber, although, of course, the wash water may contain other components than HCl. This research is along similar lines as the work of Comans and Meima [7] and Eighmy et al. [8]. In the latter work, the emphasis was, however, on the spectroscopic characterisation of fly ashes, whereas the main subject of the present paper concerns computer predictions and calculations that will be compared with experimental results in order to gain a better understanding of the leaching process. Theoretical calculations were performed using the equilibrium simulation program MINTEQA2.

2. Materials and methods

2.1. Materials and characterisation

Samples of MSWI fly ash were obtained from the Houthalen Waste Incineration Facility (Houthalen, Belgium), a municipal solid waste facility with an annual capacity of 98 000 tonnes. The fly ash was collected by a classical electrofilter.

The particle size distribution was determined with a system of sieves with variable sieve size (0, 45, 63, 100, 200, 300, 400 and 500 μm diameter).

To obtain an approximation of the total amount of every metal on the fly ash, a leaching test was conducted in a highly acid environment (18 mol HCl per kg of fly ash), and the metal concentrations in the leachate were measured by Inductively Coupled Plasma Mass Spectrometry (ICP-MS), as described later.

The total amount of CO_3^{2-} bound in the fly ash was determined by leaching the fly ash in an acid environment (1 M HCl solution), whereby, the carbonate is converted into CO_2. Nitrogen was blown through the leaching solution to remove the CO_2, which was

trapped and neutralised in a 1-M NaOH solution. The carbonate concentration was then determined by titration.

The phosphate concentration in the leaching solution was determined using the *Molybdene-blue* spectrophotometric method [9].

The total amount of chloride (the sum of the amount of chloride ions from the HCl leaching solution, and the amount that is leached from the fly ash) was determined by titration with $AgNO_3$.

2.2. Leaching experiments

A total of 100 ml HCl solution (HCl concentration ranging from 0 to 1.8 M) was added to 10 g of fly ash in a polyethylene container. The fly ash and the leaching solution were brought in contact by mechanical shaking for a period of 3 h at room temperature. After shaking, the mixture was centrifuged. Then, the final pH was measured and the solution was filtered over a glass microfibre filter (Whatman GF/C). Metal concentrations in solution were measured by Inductively Coupled Plasma Mass Spectrometry (ICP-MS). To the diluted leachate, In (internal standard) and HNO_3 were added in order to obtain a concentration for In of 100 μg/l and for HNO_3 of 2%. A total of 10 ml of this solution was measured against standards containing 100 μg/l of the relevant trace elements and 100 μg/l of In. The measurements were carried out with a Plasma Quad PQ2 + (VG-Elemental) spectrometer.

A parameter AD is defined as:

$$\mathrm{AD} = \frac{\text{amount of } H^+\text{-ions added}}{\text{mass of fly ash}} \left(\frac{\text{mol}}{\text{kg}} \right)$$

or

$$\mathrm{AD} = \frac{\text{amount of } OH^-\text{-ions added}}{\text{mass of fly ash}} \left(\frac{\text{mol}}{\text{kg}} \right).$$

In the former case, AD is given a positive value, in the latter case, a negative value. H^+-ions were added as HCl; OH^--ions as NaOH. AD was varied from -2 mol/kg to 18 mol/kg, to study the evolution of pH and metal concentrations as a function of AD.

Another parameter important in evaluating the leaching characteristics is the liquid–to–solid ratio, L:S, defined as:

$$\mathrm{L{:}S} = \frac{\text{volume of leaching } v \text{ solution}}{\text{mass of fly ash}} \left(\frac{\text{l}}{\text{kg}} \right).$$

The leaching experiments were performed with a L:S of 10 l/kg.

The redox potential was determined experimentally as a function of AD using a combined Pt–Ag/AgCl electrode.

2.3. The computer program MINTEQA2

2.3.1. Description

MINTEQA2 [10,11,12] is a geochemical model capable of calculating equilibrium aqueous speciation, adsorption, gas phase partitioning, solid phase saturation states, and

precipitation–dissolution of metals. The model uses an extensive thermodynamic database to solve the chemical equilibrium problems. In a first step, an input file is created in which the parameters of the system are specified, including pH and ionic strength, along with initial concentrations of ions (e.g. Ca^{2+}, CO_3^{2-}) or initial amount of minerals (e.g. $CaCO_3$). If the system contains elements that have two or more stable oxidation states, the redox potential must also be specified.

In MINTEQA2, a set of 'basic components' is predefined. Every chemical species (basic component, complex, ion, solid or gas) can be written as a combination of these components (e.g. the species $CaCl^+$, $CaCl_2$, etc. can all be written as a combination of the basic components Ca^{2+} and Cl^-). For each of the N aqueous species that can be formed starting from the M (basic) components in the input file, the value of the stability constant for the formation reaction is included in the database of MINTEQA2. Where literature values are available, MINTEQA2 also gives the maximum and minimum value for the stability constant. The user has the possibility to adjust the stability constants.

In a second step, MINTEQA2 solves the system of N equations iteratively, in which the unknown variables are the concentrations of M basic components and N–M other species. For each of these N–M other species, an equilibrium equation can be written using the stability constant in the database. The system is closed with the specified initial concentrations of the M basic components.

The saturation index (SI) of a solid indicates if it precipitates or not. For every mineral that can be formed starting from the basic components in the input file, SI is calculated. Minerals with negative SI are undersaturated, minerals with positive SI are oversaturated and will precipitate. For these solids, the precipitated amount is an additional unknown parameter; the system of N equations is completed with the requirement that $SI = 0$. In the output of the program, all necessary information about the equilibrium is given, such as concentrations, aqueous speciation, equilibrium pH and saturation indices of solids. Activity coefficients are calculated by the program using the Davies or Debye–Hückel equation for charged species and the Helgeson method for neutral species. The ionic strength is calculated from the speciation in the solution and then entered in the program as a fixed value. This required an iterative procedure.

MINTEQA2 allows the user to choose to exclude solids from precipitation, or to include only a limited selection of solids for which precipitation is possible. In the calculations, all solids were allowed to precipitate. This approach has the advantage that a wide range of solids is examined, whereby, more than one solid at a time can be obtained.

2.3.2. Application

MINTEQA2 was used to determine the equilibrium situation of the leaching solution as a function of pH. In a second stage, the influence of certain components of the fly ash on the equilibrium pH of the solution was examined.

Because of the complexity of the system, it is not possible to compute the equilibrium speciation of all the components in one step. Therefore, the components were separated into five different input files (Table 1). The components that do not have an influence on the specific equilibrium reactions of an input file are omitted. Components such as Na^+ and K^+ that more or less remain in solution at each pH value, as indicated by

Table 1
Subproblems in the simulation (basic components for MINTEQA2)

Subproblem	Input			Output
	Cations and neutral components	Anions	Redox couples	
Main components of the fly ash	Ca^{2+}, H_4SiO_4, Al^{3+}	SO_4^{2-}, PO_4^{3-}, Cl^-, CO_3^{2-}, F^-	–	Calcium, aluminium
Formation of carbonates, sulphates, oxides and hydroxides	Cd^{2+}, Zn^{2+}, Mg^{2+}, Ca^{2+}, H_4SiO_4	SO_4^{2-}, PO_4^{3-}, Cl^-, CO_3^{2-}, F^-	–	Cadmium, zinc, magnesium carbonate
Formation of phosphates, oxides and hydroxides	Pb^{2+}, Mg^{2+}, Ca^{2+}, H_4SiO_4	SO_4^{2-}, PO_4^{3-}, Cl^-, CO_3^{2-}, F^-	–	Lead, phosphate
Redox reactions with formation of silicates, chromates, oxides, hydroxides	Fe^{2+}, $Cr(OH)_2^+$, Mn^{2+}, Ca^{2+}, H_4SiO_4, Al^{3+}	SO_4^{2-}, PO_4^{3-}, Cl^-, CO_3^{2-}, F^-	Fe^{2+}–Fe^{3+}, Mn^{2+}–Mn^{3+}, Cr^{2+}–$Cr(OH)_2^+$, $Cr(OH)_2^+$–CrO_4^{2-}	Iron, manganese, chromium
Redox reactions with formation of sulfides, silicates, oxides,hydroxides	Ca^{2+}, H_4SiO_4, Cu^+, H_3AsO_4,Ni^{2+}	SO_4^{2-}, PO_4^{3-}, Cl^-, CO_3^{2-}, F^-	H_3AsO_3–H_3AsO_4, Cu^+–Cu^{2+}, Cr^{2+}–$Cr(OH)_2^+$, $Cr(OH)_2^+$–CrO_4^{2-}, HS^-–SO_4^{2-}	Arsenic, copper, nickel

experiments and separate MINTEQA2 calculations, are taken into account by adjusting the ionic strength and are not included as components. The ionic strength is calculated from the concentrations of the metals in solution during the experiments and varies from 0.28 at a pH of 10.8 to 3.2 at a pH 0. MINTEQA2 is less accurate at higher ionic strength, but comparison of the calculated concentrations with the experimental values is possible.

Calcium, for example, has a major influence on the lead equilibrium as both calcium and lead may form carbonates. The calcium equilibrium is on the other hand not influenced by lead, because lead is present in the fly ashes in a much lower concentration than calcium. Therefore, lead does not have to be included in the calcium input file.

In this way, the complex problem was divided into five smaller subproblems (represented in Table 1), giving complementary information on the overall equilibrium situation.

Input concentrations for each component were based on determined values for the mass fraction of every component in the leachable fraction of the fly ash, as presented in Section 3 (with L:S = 10 l/kg). When a component appears in more than one subproblem, the same input concentration was used for every problem.

Theoretical calculations were performed at the experimental operating temperature of 25°C. No gas phase and no sorption reactions were included in the MINTEQA2 input file. Contrary to the work of Eighmy et al. [8], components were not entered as finite solids but as components in solution. Oversaturated solids were allowed to precipitate.

Table 2
Composition of the fly ash

Component	g/kg fly ash
Ag	< 0.1
Al	73.0
Ca	204.2
Cd	0.3
Cl	54.0
Co	< 0.1
CO_3	22.1
Cr	0.1
Cu	0.5
F	0.6
Fe	6.3
Hg	< 0.1
K	38.7
Mg	7.9
Mn	0.7
Na	46.4
Ni	0.1
Pb	2.9
PO_4	27.0
Sn	0.1
SO_4	58.0
Zn	9.4

The pH was entered as a fixed value, ranging from 0 to 14. The subsystems generally required over a hundred iterations to reach convergence. Unless otherwise indicated, the default value for the stability constants in the MINTEQA2 input file was used.

3. Results

3.1. Characterisation of the fly ash

The composition of the leachable fraction of the fly ashes (g/kg fly ash) is presented in Table 2. This is about 70% of the total mass. Major constituents of the fly ash are aluminium and calcium. The remaining fraction (about 30%) consists mainly of silicate compounds [8,13,14].

The particle size distribution indicates that the particles are mostly smaller than 200 μm in diameter. Only 7 wt.% is larger than 200 μm. The largest fraction is retained on the sieve corresponding to the 45–63 μm fraction. This particle size distribution is similar to that of other fly ashes [15].

3.2. pH of the leaching solution

Fig. 1 shows the evolution of the final pH after extraction as a function of AD. Between acid dose 0 and 4 mol/kg, the pH decreases rapidly. Here, only small amounts of basic metal salts dissolve, so that the added acid is not neutralised. Between acid dose 4 and 12 mol/kg, the pH decreases more slowly. The added acid is consumed to neutralise the dissolving basic metal salts (buffering capacity of the fly ash). When using an AD > 12 mol/kg, the amount of basic salts is insufficient to neutralise the added acid giving a logarithmic decrease in the pH.

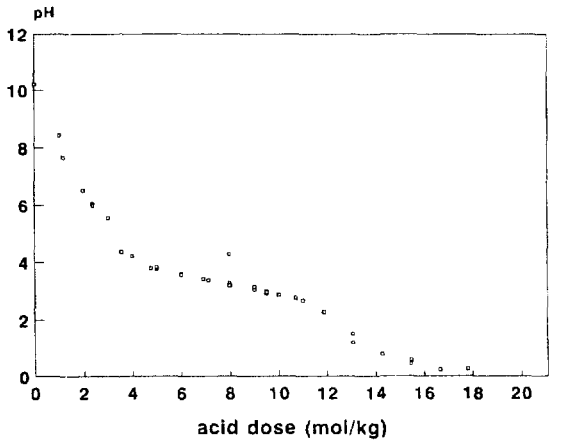

Fig. 1. Final pH as a function of the acid dose (L:S = 10 l/kg, extraction time = 3 h).

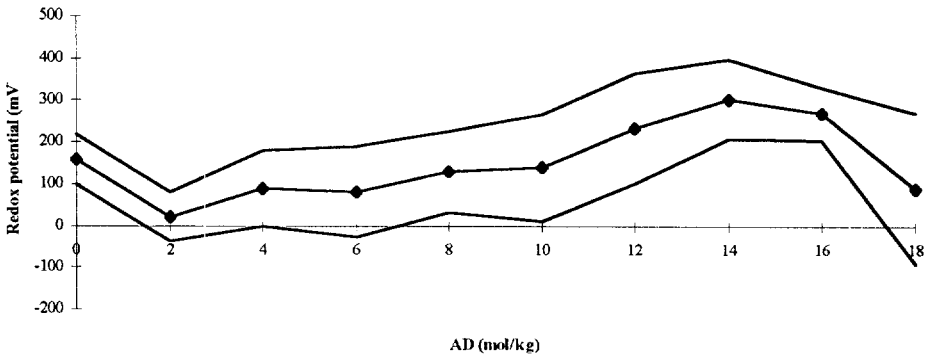

Fig. 2. Redox potential of the leaching solution.

3.3. Redox potential

The results of the determination of the redox potential are presented in Fig. 2. These values were obtained as an average of 11 measurements with a standard deviation ranging from 60 mV to 130 mV. These experimental results are comparable with the calculated values.

3.4. Simulation

3.4.1. Theoretical solubility

3.4.1.1. Zinc. In Fig. 3, the *leaching diagram* for zinc is presented. The bold curve represents calculated values of the amount of zinc leached per gram of fly ash as a function of pH. These were obtained by multiplying the MINTEQA2 output concentra-

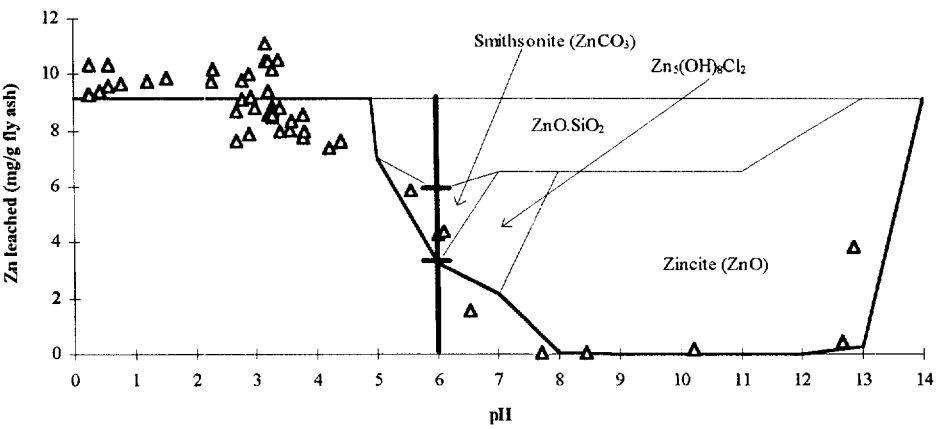

Fig. 3. Leaching diagram of zinc (△ experimental values; ———— calculated).

tions with L:S. Experimental results are given, for comparison, in the same figure.

For each pH value, the leaching diagram represents the quantitative partitioning between the different phases. The indicated minerals are the controlling solids at the specific pH value. The MINTEQA2 input file includes the components as species in solution, not as finite solids. At equilibrium, more than one mineral may be precipitated. When starting from finite solids, several solids must be excluded to avoid phase rule violations.

At pH 6, for example, about one third of the total zinc concentration remains in solution (Fig. 3), whereas, one third is precipitated as smithsonite and one third as $ZnO \cdot SiO_2$.

Other controlling solids are $Zn_5(OH)_8Cl_2$ (pH 6 to 8) and ZnO (pH 7 to 13).

At low pH, the theoretical curve is flat, which means that the equilibrium concentration is determined by the maximum amount of zinc that leaches from the fly ashes. At higher pH values, the concentration at equilibrium is determined by solubility restrictions. At pH 5, the solubility of zinc decreases due to the precipitation of zinc silicate; at pH 8, different zinc minerals occur and no more zinc remains in solution. At pH > 13, zinc solubility increases again, due to the formation of hydroxide complexes. For a better agreement between experimental and calculated values, the logarithm of the stability constant (log K) for smithsonite is taken as 9.92, whereas, the suggested value is 10.0. This chosen value lies between the minimum and maximum values found in literature which are, respectively, 9.82 and 10.81.

The theoretical predictions are in excellent agreement with the experimental data.

3.4.1.2. Aluminium and calcium. The simulation results for aluminium are given in Fig. 4. Between a pH of 4 and 13, aluminium is precipitated as diaspore (AlOOH). At a pH higher than 13, the solubility of diaspore increases. The log K value for diaspore was taken as -7.397 [16]. The leaching diagram is in very good agreement with the experimental values. However, considering the high concentration of aluminium on the fly ashes, aluminium might also play a role in the precipitation of calcium as an alumino-silicate compound. The leaching diagram for calcium is given in Fig. 5. The composition of the silicate structures, determined in Ref. [8] with XRPD (X-ray Powder Diffraction) and solid-phase dissolution, was not obtained in the calculations. Gypsum

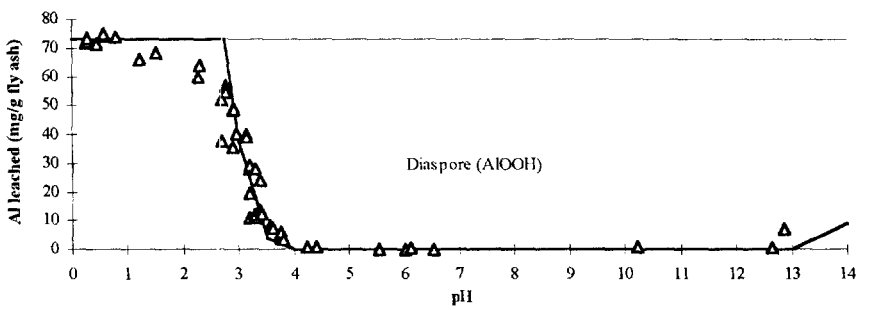

Fig. 4. Leaching diagram of aluminium.

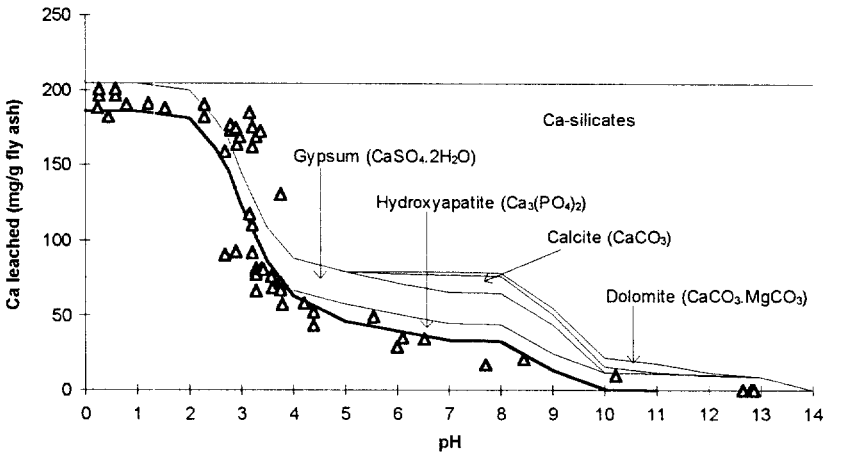

Fig. 5. Leaching diagram of zinc.

was found to be a controlling solid over the whole pH range; at high pH values, hydroxyapatite, calcite and dolomite appear as controlling solids.

3.4.1.3. Lead. The leaching diagram for lead is given in Fig. 6. Only one controlling solid occurs: chloropyromorphite at a pH lower than 9, and $Pb(OH)_2$ at high pH values. The log K value for chloropyromorphite was taken as 92.27 (value suggested by MINTEQA2 is 84.43, minimum value is 34.51, no maximum value indicated). The log K value of $Pb(OH)_2$ was taken as -10.15 (value suggested by MINTEQA2 is -8.15, minimum value -13.63, no maximum value indicated).

3.4.1.4. Cadmium. Theoretical calculations and experimental determination of the cadmium equilibrium are in good agreement (Fig. 7) when the log K of otavite is taken as 12.45 (value suggested by MINTEQA2 is 13.74, minimum value 11.21, maximum value 13.81). Under very basic conditions, $Cd(OH)_2$ occurs.

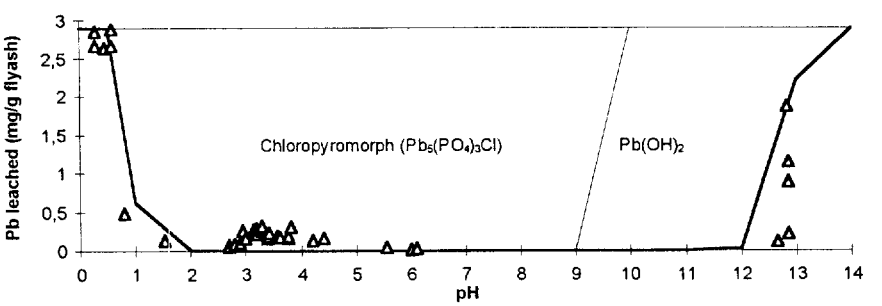

Fig. 6. Leaching diagram of lead.

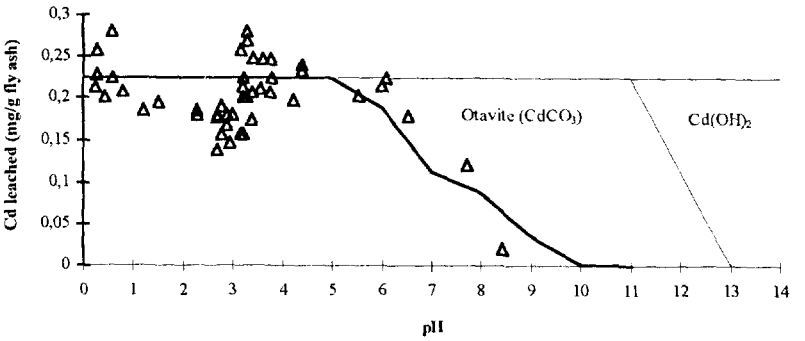

Fig. 7. Leaching diagram of cadmium.

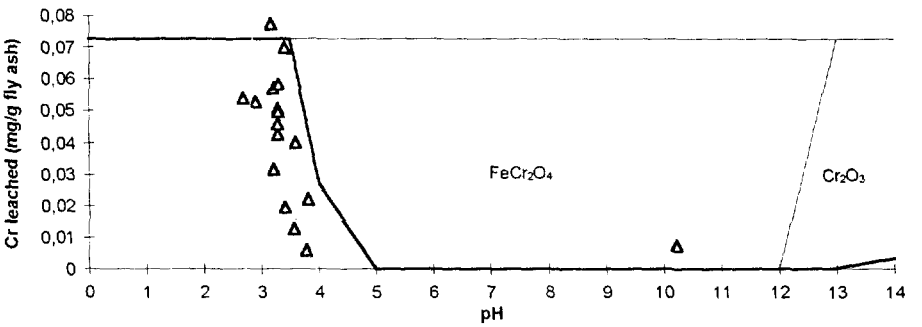

Fig. 8. Leaching diagram of chromium.

3.4.1.5. Chromium, copper and iron. Chromium (Fig. 8) is precipitated as $FeCr_2O_4$, and Cr_2O_3 if pH > 12. For copper (Fig. 9), sulfidic minerals (covellite, djurleite and chalcocite) are found as well as oxidic minerals (cuprite). Hematite is the most important controlling solid for iron (Fig. 10). Small amounts of Ca-nontronite and $FeCr_2O_4$ occur.

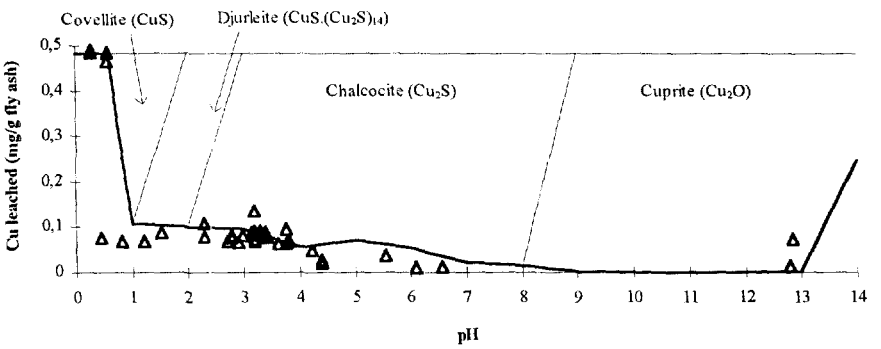

Fig. 9. Leaching diagram of copper.

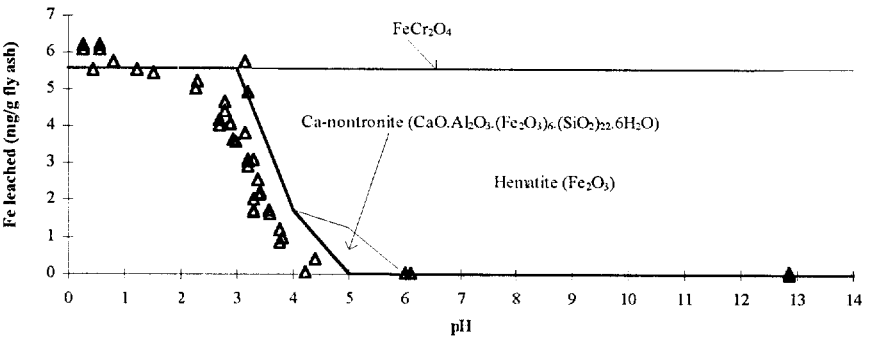

Fig. 10. Leaching diagram of iron.

For iron and chromium, the calculated curve is shifted by about 0.5 pH to the right compared to the experimental one. This difference remains unexplained.

3.4.2. Equilibrium pH

As discussed in the previous chapter, the pH of the leaching solution is an important parameter in determining the solubility of a metal. Therefore, modelling was also applied to predict the equilibrium pH of fly ash leached with an acid solution of given AD. A new MINTEQA2 input file was created, comprising finite solids which are assumed to be present in the leachable fraction of the fly ash [6,13]: CaO, $CaCO_3$, $CaSO_4$ and $CaCl_2$; Al_2O_3; NaCl and Na_2O; etc.

So far, the pH was entered as a fixed value in the MINTEQA2 input file. Now, the initial H^+-concentration of the acid leaching solution is entered in the MINTEQA2 input file. When the fly ash is brought in contact with the acid solution, basic oxides will dissolve causing an increase of the pH, giving the fly ash a certain buffering capacity. The equilibrium pH after dissolution of basic oxides was calculated by MINTEQA2 for various values of AD.

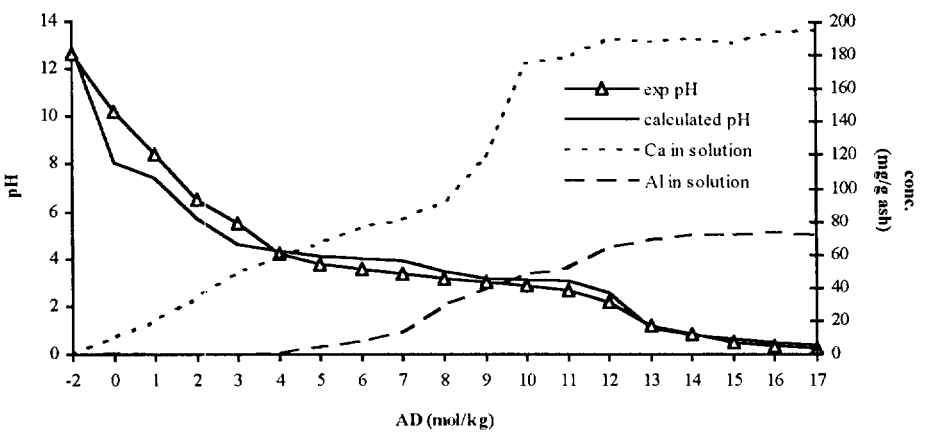

Fig. 11. Experimental and calculated pH, calcium and aluminium concentration as a function of the AD.

It was found by varying the amount of the solids one at a time that the parameters that have an influence on the equilibrium pH are AD and the leachable amounts of $CaCO_3$, CaO and Al_2O_3. The variation of pH is mainly related to dissolution of aluminium and calcium oxides.

Fig. 11 compares experimental and calculated pH values and shows the dissolved amount of calcium and aluminium. Up to a AD of 4 mol/kg, aluminium oxides do not dissolve and CaO is the main neutralising basic oxide. At a AD higher than 10 mol/kg, calcium is nearly completely dissolved and Al_2O_3 is the main neutralising basic oxide. Once the soluble amount of aluminium is in solution, the buffering capacity of the fly ash is consumed and increasing the AD leads to a logarithmic decrease of the pH.

The agreement between experimental and calculated pH is excellent.

4. Applications

4.1. Fly ash with a different composition—addition of complexing agents

If the overall composition of fly ash from a different source is known, the leaching behaviour can be easily predicted by adjusting the input concentrations for the MINTEQA2 calculations.

Another possible application of the simulation program is prediction of the leaching behaviour when complexing agents such as EDTA are added. In Fig. 12, the calculated solubility of lead in the leaching solution is given with and without addition of 0.26 g Na_2EDTA/g fly ash, and compared with experimental values for lead leachability with addition of EDTA.

From the figure, it can be seen that the solubility of lead increases dramatically in the pH-range from 1 to 7 by the addition of EDTA. The agreement between calculated and experimental results is excellent.

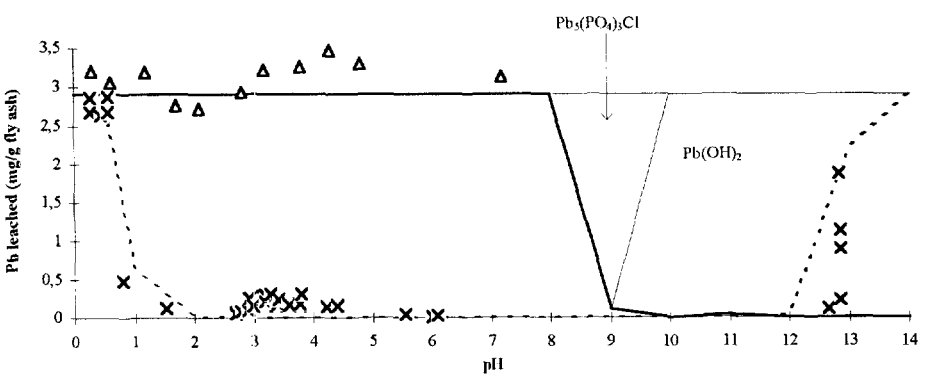

Fig. 12. Simulation of the leaching behaviour of lead with addition of EDTA (△ experimental values; ——— calculated; — calculated without EDTA addition; x experimental without EDTA addition).

Table 3
Precipitation limit for zinc

L:S (l/kg)	5	8	10	12	15	20
pH of precipitation	4.8	4.9	4.9	4.9	4.9	5.0

4.2. Optimisation of L:S

L:S is an important parameter, the influence of which can be examined with the simulation model. L:S must be kept as low as possible as it determines the size of the plant (leaching reactor and following equipment, such as centrifuges and filters) needed to process a given amount of fly ash. L:S also determines the concentration of the leached metals in solution. If less leaching liquid is used for a given amount of fly ashes, a higher metal concentration may be obtained. If recovery is considered, this concentration must be as high as possible, in order to obtain a high yield.

On the other hand, L:S has a lower limit, because in order to obtain efficient leaching no precipitation may occur. Precipitation at lower L:S when using the same washing liquid can be caused by the following (interdependent) reasons.

1. AD decreases: if washing liquid with a given pH is used, AD is proportional to L:S ($AD = 10^{-pH}$ L:S).
2. Metals precipitate at a lower pH when the concentration in the solution is higher (shift in leaching diagram). As an example, the limit pH where zinc starts to precipitate is indicated in Table 3.
3. The equilibrium pH for the same AD is higher as a larger amount of basic oxides dissolves. In Fig. 13, the pH of the leaching solution at equilibrium is represented as a function of AD for L:S = 5, 10, 15. This was done by adjusting AD and the concentrations of aluminium and calcium oxides in MINTEQA2.

Table 3 and Fig. 13 indicate that the dependence of the leaching diagram and the equilibrium–pH from L:S is not high. When using a washing liquid with fixed pH, L:S has an influence on the equilibrium mainly through a change of AD.

For a given problem, the simulation model can be used to optimise L:S in an iterative process, as is visualised in the algorithm below. Influence of the variation of the

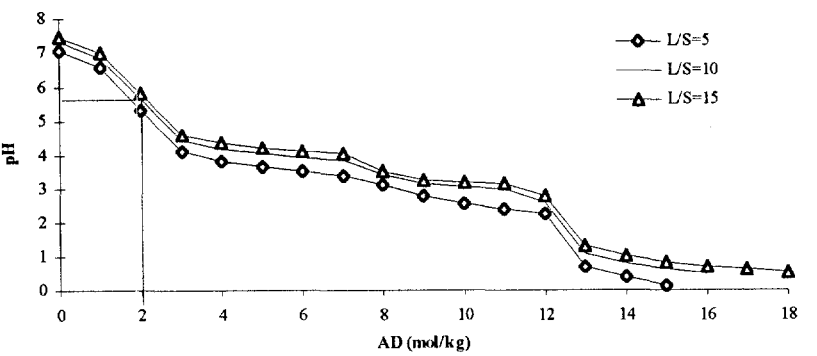

Fig. 13. pH of the leaching solution as a function of AD.

equilibrium–pH and the leaching diagram are included in this algorithm. A safety margin Δ(pH), defined as the difference between theoretical precipitation limit and actual equilibrium pH, is included to account for fluctuations in the leaching process, e.g. the pH of the washing liquid.

Algorithm:

1. Define pH* of washing liquid
2. Choose safety margin Δ(pH)
3. Initial value for L:S
   Repeat
4. Calculate AD = 10^{-pH*} L:S
5. Calculate equilibrium–pH → pH_e
6. Calculate precipitation–pH → pH_p
7. if $pH_e > pH_p$, then [precipitation] choose higher L:S;
   if $pH_p > pH_e > pH_p - \Delta(pH)$, then [safety margin] choose higher L:S;
   if $pH_e < pH_p - \Delta(pH)$, then [metals still in solution, too much acid used] choose lower L:S
   until $pH_e = pH_p - \Delta(pH)$ [optimum]

The pH of the washing liquid coming from an exhaust gas cleaning plant of a municipal waste incinerator is generally approximately 0.7. The safety margin Δ(pH) can, e.g., be taken as 0.2. At L:S = 10, a pH of 0.7 implies that AD ≈ $10^{-0.7} \cdot 10$ mol/kg ≈ 2 mol/kg.

The pH of the leaching solution at equilibrium can now be read from Fig. 13 ($pH_e \approx 5.7$).

Then, the chemical equilibrium of the solution is calculated with concentrations at the specified L:S. If the considered metals are still in solution, the iteration is repeated with a lower L:S. For zinc, these results are presented in Table 3. At a pH_e (equilibrium pH) of 5.7, zinc is precipitated.

The calculations must be repeated with a higher L:S to keep zinc in solution. If L:S is taken as 15, AD is about 3. The equilibrium pH is then 4.6 and the precipitation pH is 4.9. The safety margin of 0.2 pH units is respected; this means that L:S = 15 is an appropriate value.

5. Discussion

The simulation results can be compared with those of Eighmy et al. [8], Van der Hoek and Comans [17], Comans and Meima [7] and Mulder [4]. In the second study, the precipitation behaviour of calcium in the leachate of a MSWI bottom ash was examined with MINTEQA2. Gypsum was found to be the controlling solid in acidic and neutral conditions, the mineral ettringite in basic conditions. The leaching diagram calculated in the present research is much more complex due to the generalised approach without excluding any solids. To visualise the complex equilibrium clearly for every pH value, a leaching diagram with a linear scale is used instead of the usual logarithmic scale.

Van der Hoek and Comans [17] found indications that sorption processes could play a

role for certain trace elements. The experiment of Mulder [4] shows comparable extraction efficiencies for cadmium, copper, lead and zinc.

The study conducted by Eighmy et al. [8] differs in some essential points from the present simulation, although a similar leaching process for fly ashes was used. The main difference was the use of a HNO_3 instead of a HCl leaching solution. Other differences are the composition of the fly ashes, the L:S ratios used in experiments, and the MINTEQA2 calculation approach, starting from solids instead of components in solution. Also, the main objective in [8] was the experimental characterisation of the different mineral phases, while calculations were used to verify the results.

In spite of these differences, the results of Eighmy et al. [8] are well comparable to the leaching diagrams obtained in this study. For *zinc*, precipitation of smithsonite and $ZnSiO_3$ was also calculated in Ref. [8], while zincite (ZnO) was detected experimentally by X-ray Photoelectron Spectroscopy (XPS) and solid-phase dissolution. Furthermore, a chloride containing mineral was detected with XPS and Secondary Ion Mass Spectroscopy (SIMS). These results agree with the leaching diagram of Fig. 3 to a great extent.

In contrast, the leaching diagram for *chromium* (Fig. 8) differs from the results of Eighmy et al., where $PbCrO_4$ is found instead of $FeCr_2O_4$. This may be explained by the difference in redox potential during leaching. Moreover, the fly ash examined by Eighmy et al. contains less iron and considerably more lead. Differences in redox potential could also explain the different results for copper (Fig. 9) and iron (Fig. 10), where Eighmy et al. only found $Fe(OH)_3$ and $Cu(OH)_3$.

For *aluminium*, *calcium*, *lead* and *cadmium*, the results of Eighmy et al. [8] are not essentially in contradiction with the leaching diagrams in Figs. 4–7.

In comparison with Refs. [7,8], a more detailed simulation of the leaching process is obtained in the present study. An important improvement in understanding the leaching process is the simulation of the pH as a function of AD. This part plays a key role in controlling the process by predicting the equilibrium state after leaching.

6. Conclusion

Solubility and precipitation of heavy metals are the main elements of the leaching process. Leaching diagrams obtained by simulation calculations are useful means to obtain a clear picture of the precipitation equilibria for different metals. At given equilibrium pH of the leaching solution, the leaching diagrams indicate which metals are in solution, and which minerals are precipitated. The leaching diagrams vary slightly with changing L:S.

During the leaching process, the pH of the leaching solution increases as basic oxides dissolve. The equilibrium pH is determined by AD, L:S, and the amount of $CaCO_3$, CaO and Al_2O_3 on the fly ash.

By comparison with experimental data, the simulation program has proven to give reliable results although the model only represents equilibrium-limited leaching. As an application, the influence of the addition of complexing agents was examined. In the

case of lead, a dramatic increase in solubility was obtained with addition of EDTA. The simulation program is also useful for the determination of an optimum value for L:S.

Because the results obtained by calculation are in good agreement with experimental results and other studies, it indicates that the simulation of the leaching behaviour can be extended to fly ashes with different compositions, or to other leaching conditions.

Less experiments are needed if the simulation is used: only leaching tests with aqua regia or a high AD. Under these circumstances, the total leachable amount of the metals can be measured, as well as the anions presents on the fly ash. Experimental work is reduced because leaching tests with variable AD become superfluous.

Acknowledgements

Grateful acknowledgement is made to R. Swennen for critically reading the manuscript. The authors also wish to thank the IWT (Vlaams Instituut voor de bevordering van het wetenschappelijktechnologisch onderzoek in de industrie) for support.

References

[1] D. Wille, G. de Boeck, Inventarisatie Huishoudelijke Afvalstoffen in Vlaanderen in 1994, Productie, Inzameling en Verwerking, Openbare Afvalstoffenmaatschappij voor het Vlaamse Gewest, Publicatie nr. D/1996/5024/4, April 1996.

[2] R. Senelle, J. Dujardin, M. Van Damme, VLAREM II, Die Keure La Charte, Brugge, 1995.

[3] J. Vehlow, H. Brown, K. Horch, A. Merz, J. Schneider, L. Stieglitz, H. Vogg, Semi-technical demonstration of the 3R process, Waste Manage. Res. 8 (1990) 461–672.

[4] E. Mulder, Pre-treatment of MSWI-fly ash for useful application, Waste Manage. 16 (1-3) (1996) 181–184.

[5] Y. Gong, D.W. Kirk, Behaviour of municipal solid waste incinerator fly ash, J. Hazard. Mater. 36 (1994) 249–264.

[6] P. Van Herck, C. Vandecasteele, D. Wilms, Characterisation of fly ash from municipal waste incineration and study of the leaching in view of metal removal, Proceedings of Solid Waste Management: Thermal Treatment and Waste-to-Energy Technologies, Washington, 1995, Air and Waste Management Association, Pittsburgh, pp. 723–728.

[7] R.N.J. Comans, J.A. Meima, Modelling Ca-solubility in MSWI bottom ashes leachates, Elsevier, Proceeding of the international conference on environmental implications of construction materials and technology developments, Maastricht, The Netherlands, 1–3 June, 1994, pp. 103–110.

[8] T.T. Eighmy, J. Dykstra, J.E. Krzanowski, D.S. Domingo, D. Stämpfli, J.R. Martin, P.M. Erickson, Comprehensive approach towards understanding element speciation and leaching behaviour in municipal solid waste incineration electrostatic precipitator ash, Environ. Sci. Technol. 29 (1995) 629–646.

[9] L.S. Clesceri, A.E. Greenberg, R.R. Trussell, Standard methods for the examination of water and wastewater, 17th edn., part 4, American Public Health Association, Washington, DC, 1989, 177–178.

[10] J.D. Allison, D.S. Brown, K.J. Novo-Gradac, MINTEQA2/PRODEFA2, A Geochemical Assessment Model for Environmental Systems: User's Manual, Environmental Research Laboratory, US EPA, Athens, GA, 1991.

[11] A.R. Felmy, D.C. Girvin, E.A. Jenne, MINTEQ: A Computer Program for Calculating Aqueous Geochemical Equilibria, U.S. EPA Project 600/3-84-032, US EPA, Washington, DC, 1994.

[12] MINTEQA2, version 3.11, Environmental Research Laboratory, Office of Research and Development, US Environmental Protection Agency.

[13] C.S. Kirby, J.D. Rimstidt, Mineralogy and surface properties of municipal solid waste ash, Environ. Sci. Technol. 27 (1993) 652–660.

[14] R. Derie, Les cendres volantes des incinérateurs d'ordures ménagères, Struct. Reactivité Chim. Nouvelle 10 (37) (1993) 1091–1097.

[15] International Ash Working Group, An international perspective on characterisation and management of residues from municipal solid waste incineration, Summary Report, International Ash Working Group, 1994.

[16] O. Knacke, O. Kubaschewski, K. Hesselmann, Thermochemical properties of inorganic substances, 2nd edn., Springer-Verlag/Verlag Stahleisen, Berlin and Heidelberg, 1991.

[17] E.E. Van der Hoek, R.N.J. Comans, Speciation of As and Se during leaching of fly ash, Environmental Aspects of Construction with Waste Materials, Elsevier, Proceeding of the International Conference on Environmental Implications of Construction Materials and Technology Developments, Maastricht, The Netherlands, 1–3 June, 1994, pp. 467–476.